Electronic Supplementary Material (ESI) for Nanoscale.

Supporting Information

Evidence of oxygen vacancy mediated ultrahigh SERS sensitivity of Niobium Pentoxide nanoparticles through defect engineering: Theoretical and experimental studies

Sirsendu Ghosal[1], Abhilasha Bora[1] and P. K. Giri[1, 2*]

[1]*Department of Physics, Indian Institute of Technology Guwahati, Guwahati 781039, India*

[2]*Centre for Nanotechnology, Indian Institute of Technology Guwahati, Guwahati 781039, India*

* Corresponding author; email: giri@iitg.ac.in

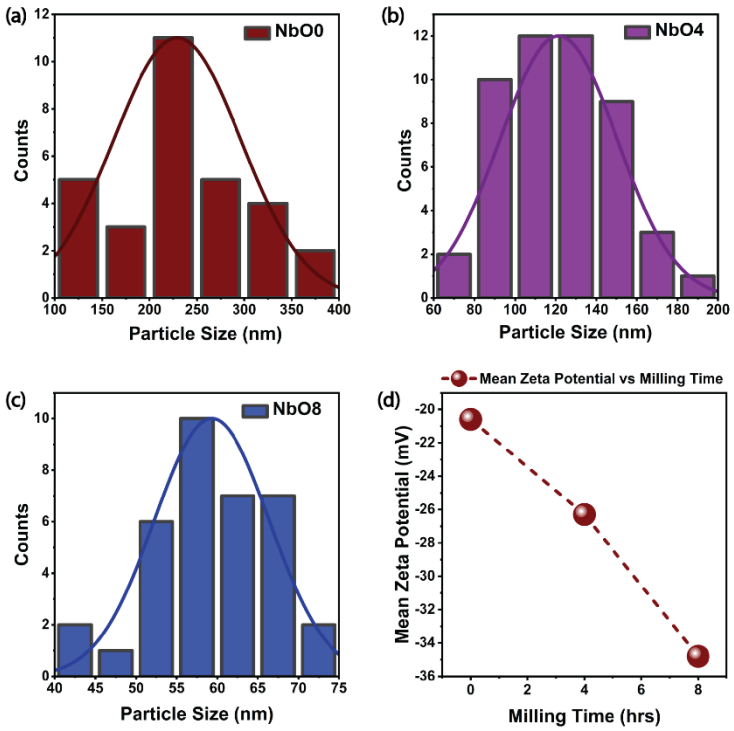

Fig. S1: Average particle size distribution of (a) 0 hr, (b) 4 hr and (c) 8 hr milled Nb_2O_5 samples (d) The zeta potential value of various milled powders in aqueous solution.

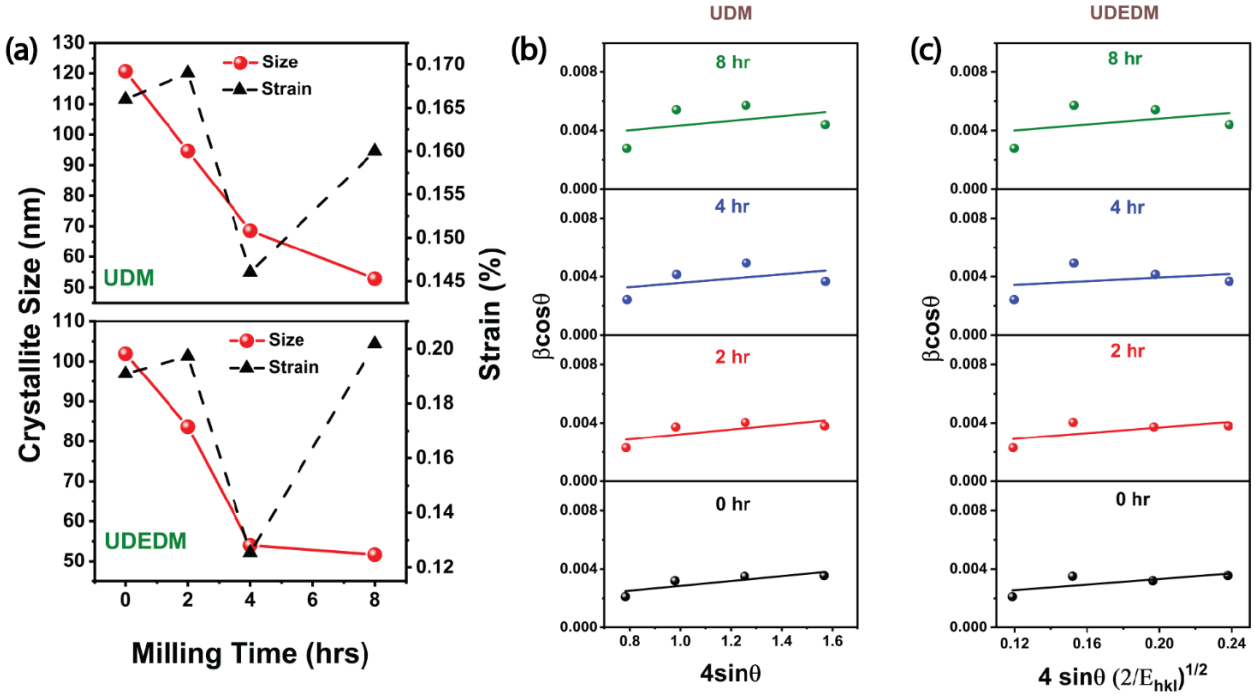

Fig. S2: (a) Calculation of the average crystallite size and strain with UDM and UDEDM models, (b) UDM fitting of the XRD data for 0, 2, 4 and 8 hr milled samples. (c) UDEDM fitting of the same.

Table T1: The XRD peak positions and the corresponding FWHM values for (001) peak of Nb_2O_5 after milling for different durations.

Milling time (hrs)	(001) peak position (2θ in deg)	FWHM (degree)	Crystallite size (nm)		Particle size from TEM image (nm)
			UDM	UDEDM	
0	22.57	0.118	120.6	101.94	228
2	22.64	0.119	94.61	83.67	-
4	22.75	0.123	68.60	54.01	121
8	22.72	0.142	52.83	51.70	59

Table T2: Comparison of the reported Raman band positions of Methylene Blue (MeB) and our SERS spectrum.

Sr. No.	Wavenumber (cm^{-1}) (Reported)	Peak assignment	Our SERS spectrum (cm^{-1})
1.	949	C-H in plane bending	950
2.	1067	C-H in plane bending	1075
3.	1181	C-N streching	-
4.	1301	β (CH); v $(C\text{-}N)_{Ring}$	1297
5.	1392	C-H in plane ring deformation	1390
6.	1444	C-N asymmetric streching	-
7.	1618	C-C ring streching	1625

Section S1.

Calculation of SERS Enhancement Factor:

The SERS enhancement factor (EF) was calculated according to the formula:[1,2]

$$EF = \frac{I_{SERS}}{N_{SERS}} \times \frac{N_{Bulk}}{I_{Bulk}} \quad (1)$$

$$N_{SERS} = CVN_A A_{Raman}/A_{Sub} \quad (2)$$

$$N_{Bulk} = \rho h A_{Raman} N_A / M \quad (3)$$

Here I_{SERS} and I_{Bulk} are the highest Raman peak intensities of the most intense peak of the dye molecule of the SERS spectra and the Non-SERS spectra. In our case, we consider the 1625 cm^{-1} of the MeB molecule for subsequent calculations. N_{SERS} and N_{Bulk} are the average number of analyte molecules present in the scattering area of SERS and the non-SERS substrate respectively. C is the molar concentration of the analyte solution that is drop-casted over the SERS substrate and V is the volume being drop-casted. N_A is the Avogadro number and ρ is the density of the bulk MeB ($\rho = 1.757\ gm/cm^3$) and molecular weight of the MeB (M = 319.85 gm/mol) is denoted by M. A_{Raman} is the area of the spot being irradiated by the excitation laser ($1\ \mu m$). The effective area of the substrate A_{Sub} is calculated from the diameter of the circle when the drop-casted MeB solution ($5\ \mu L$) forms a circular region of diameter 10 mm on the SERS substrate. h is the confocal depth of the excitation laser and is estimated as follows. The formula to calculate laser spot diameter W_0 is given as

$$\text{Laser spot diameter, } W_0 = \frac{1.22\lambda}{NA} \quad (4)$$

Where NA is the numerical aperture of the objective lens, for 100X objective NA is 0.90. The wavelength of the excitation laser 532.8 nm. Thus W_0 is calculated 722.24 nm. Now, the focal depth is calculated as

$$h = \left(\frac{2\pi}{\lambda}\right) W_0^2 \tag{5}$$

From the above equation the confocal depth is calculated 6.16 µm. From equation (2) and (3) we calculate

$$\frac{N_{Bulk}}{N_{SERS}} = \frac{\rho h A_{subs}}{MCV} \tag{6}$$

The calculation of the enhancement factor for different concentrations of Methylene Blue on NbO8 substrate is summarized in Table T3.

Table T3: Calculated SERS enhancement factors (EF) for different concentrations of MeB on NbO8 substrate with 532 nm excitation.

Sr. No.	MeB concentration (M)	$\frac{N_{Bulk}}{N_{SERS}}$	$\frac{I_{SERS}}{I_{Bulk}}$	EF
1	10^{-4} M	5315.27	84.98	4.51×10^5
2	10^{-5} M	53152.78	43.63	2.31×10^6
3	10^{-6} M	531527.81	12.59	6.69×10^6
4	10^{-7} M	5315278.14	2.74	1.45×10^7
5	10^{-8} M	53152781.43	0.97	5.15×10^7

Table T4: Calculated SERS enhancement factors (EF) for MeB (10^{-4} M) on NbO0, NbO2, NbO4 and NbO8 substrate with 532 nm excitation wavelength.

Sr. No.	Milling time (hrs)	$\frac{N_{Bulk}}{N_{SERS}}$	$\frac{I_{SERS}}{I_{Bulk}}$	EF
1	0 hr	5315.27	35.77	1.90×10^5
2	2 hr	5315.27	40.21	2.13×10^5
3	4 hr	5315.27	53.63	2.85×10^5
4	8 hr	5315.27	84.98	4.51×10^5

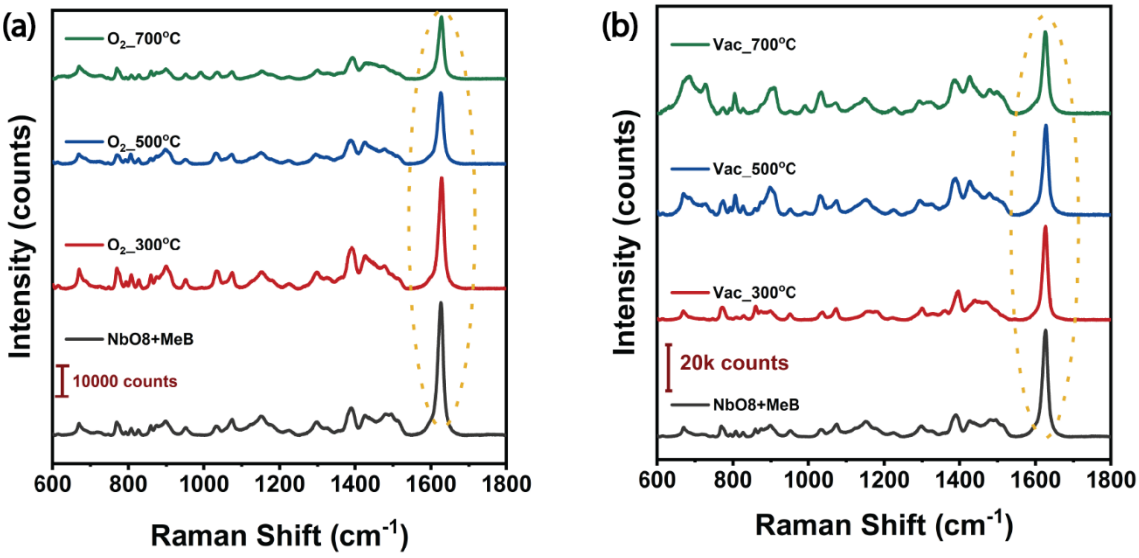

Fig. S3: Evolution of the SERS spectra of MeB (10^{-4} M) on annealed NbO8 after annealing in (a) oxygen atmosphere and (b) vacuum, at different annealing temperatures.

Table T5: Calculated enhancement factors (EF) for MeB (10^{-4} M) on NbO8 substrate annealed at different temperatures and in different annealing environments.

Sr. No.	Annealing Temp.	$\frac{I_{SERS}}{I_{Bulk}}$ (Vacuum)	$\frac{I_{SERS}}{I_{Bulk}}$ (O_2 atmosphere)	EF (Vacuum)	EF (O_2 atmosphere)
1	NIL	84.98	84.98	4.51×10^5	4.51×10^5
2	300˚C	74.69	71.05	3.96×10^5	3.77×10^5
3	500˚C	71.69	45.67	3.81×10^5	2.42×10^5
4	700˚C	65.48	39.84	3.48×10^5	2.11×10^5

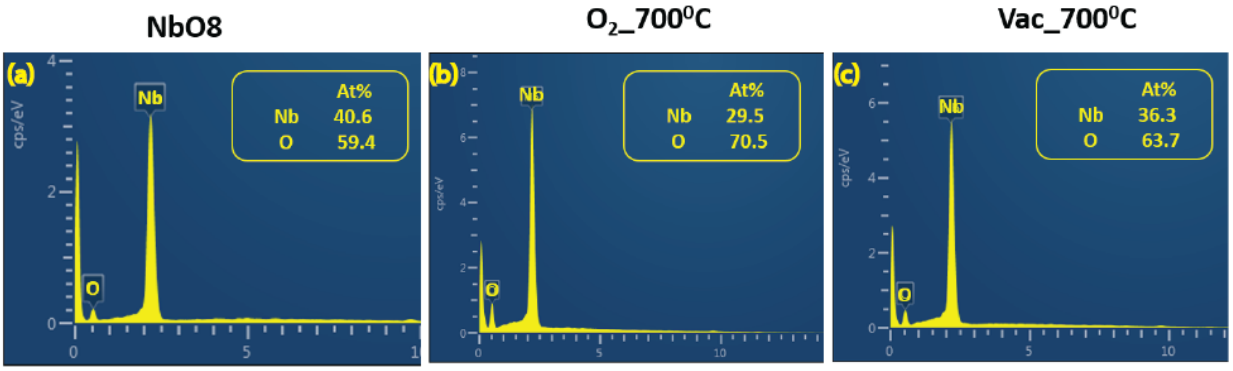

Fig. S4: EDX spectra with atomic percentage for (a) 8 h milled sample before annealing, and (b) after annealing in O_2 atmosphere at 700^0 C, and (c) after annealing in vacuum at 700^0 C.

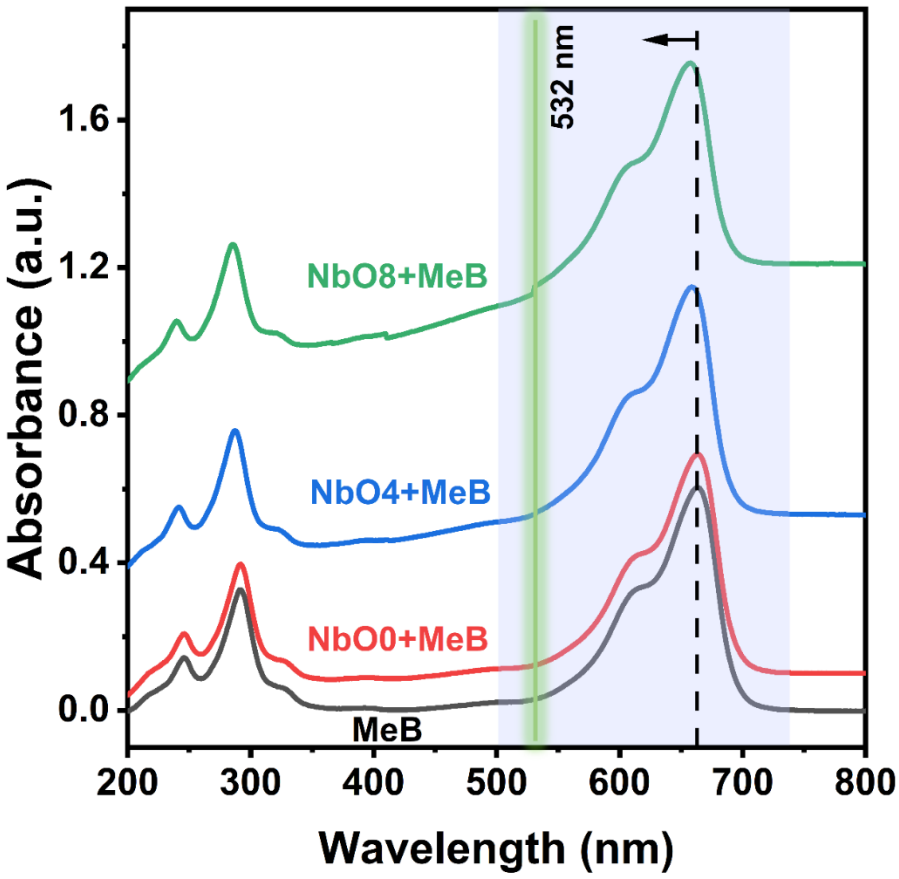

Fig. S5: Absorption spectra of 10^{-5} M MeB solution modified with different Nb_2O_5 powders milled for 0, 4 and 8 hrs, respectively.

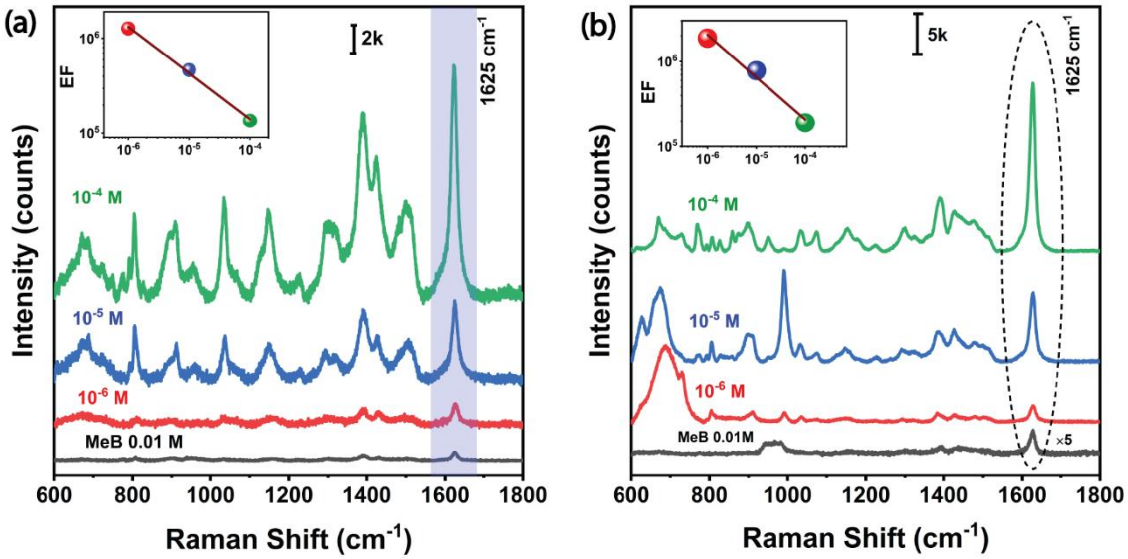

Fig. S6: (a) SERS detection of MeB molecule with different concentrations on NbO8 substrate under 633 nm excitation; the inset shows concentration vs. enhancement factors. (b) SERS detection of MeB molecule at different concentrations on NbO0 substrate; the inset shows the corresponding EF vs. concentration plot.

Section S2:

Mechanism and detailed calculation for the contribution of photo-induced charge transfer (PICT) mechanism in defect enriched semiconductor-molecule system:

The contribution of the photo-induced charge transfer (PICT) to the molecule polarization tensor was explained according to theory of Herzberg-Teller mechanism based on the vibronic coupling of the zero-order Born-Oppenheimer states. This calculation for semiconductor-molecule system without considering the defects is followed from the work of Lombardi and Wang.[3] However, in this case we will consider the defects energy levels of the semiconductor and how it couples with the molecular energy states to have a better insight into the mechanism. We denote the defect energy states by $|V>$ and the excited LUMO states of the molecule by $|L>$, while we consider two different vibronic levels of the HOMO of the molecule as $|J>$ and $|G>$ respectively.

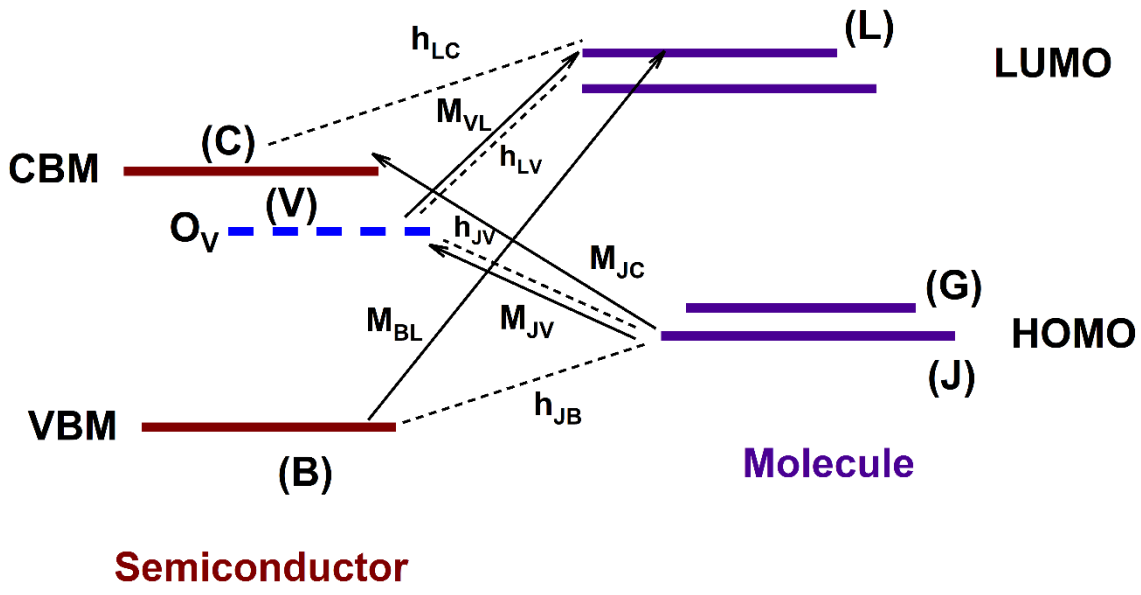

Fig. S7: Schematic of the charge transfer processes in a defect-rich semiconductor-molecule system. Refer to text for more details.

The intensity of a Raman transition is derived from the molecular polarizability tensor according to the expression.

$$I_{Raman} = [\frac{8\pi(\omega_0 \pm \omega_{IF})^4 . I_0}{9c^4}] \sum \alpha_{\rho\sigma}^2 \quad (7)$$

Where I_0 is the intensity of the incident laser beam with frequency ω_0 and ω_{IF} is the molecular transition frequency between two vibronic levels of the ground state of the molecule. Now, the polarizability tensor $\alpha_{\rho\sigma}$ is defined as

$$\alpha_{\sigma\rho} = \sum_{L \neq J,G} (\frac{<J|\mu_\sigma|L><L|\mu_\rho|G>}{E_L - E_J - \hbar\omega_0} + \frac{<J|\mu_\rho|L><L|\mu_\sigma|G>}{E_L - E_G + \hbar\omega_0}) \quad (8)$$

As stated earlier, K represents all the other states in LUMO of the molecule, μ is the dipole moment operator and ρ and σ are the incident and the scattered polarization direction in space (X, Y, Z). Now using the zero order Born-Oppenheimer approximation and following the work of Lombardi and Wang, all the vibronic states (J, G, L) can be represented as products of electronic and vibrational wave functions as

$$|J> = J_e > |j>, \quad |L> = L_e > |l>, \quad |G> = G_e > |g> \quad (9)$$

Where the subscript *e* represents a purely electronic state, and vibrational states were represented by lowercase letters. According to the Hertzberg-Teller theory it is understood that even a very small vibration also can cause mixing of zero order Born-Oppenheimer states. And the vibronic functions in a defect rich semiconductor-molecule system can be written as

$$|L_e> = |L_e, 0> + \sum_C \lambda_{LC} Q |C_e, 0> + \sum_V \lambda_{LV} Q |V_e, 0> \quad (10)$$

$$|J_e> = |J_e, 0> + \sum_B \lambda_{JB} Q |B_e, 0> + \sum_V \lambda_{JV} Q |V_e, 0> \quad (11)$$

$$\lambda_{LC} = \frac{h_{LC}}{(E_L^0 - E_C^0)} = h_{LC}/\omega_{LC} \qquad \lambda_{LV} = \frac{h_{LV}}{(E_L^0 - E_V^0)} = h_{LV}/\omega_{LV} \quad (12)$$

$$\lambda_{JB} = \frac{\lambda_{JB}}{(E_J^0 - E_B^0)} = h_{JB}/\omega_{JB} \qquad \lambda_{JV} = \frac{\lambda_{JV}}{(E_J^0 - E_V^0)} = h_{JV}/\omega_{JV} \quad (13)$$

$$h_{LC} =< L_{e,}0 \left|\frac{\partial H_{eN}}{\partial Q}\right| C_{e,}0 > \qquad h_{LV} =< L_{e,}0| \frac{\partial H_{eN}}{\partial Q} |V_{e,}0 > \qquad (14)$$

$$h_{JB} =< J_{e,}0 \left|\frac{\partial H_{eN}}{\partial Q}\right| B_{e,}0 > \qquad h_{JV} =< J_{e,}0| \frac{\partial H_{eN}}{\partial Q} |V_{e,}0 > \qquad (15)$$

Where the subscript zero refers to the zero-order Born-Oppenheimer states, H_{eN} is the electron-nuclear attraction term in the Hamiltonian, evaluated at the equilibrium positions (0). Whereas, the electronic states lying in the valence and the conduction bands denoted by $|B_e >$ and $C_e >$ respectively and h_{LC} is the coupling matrix element representing the degree of which a particular vibration Q can mix states C_e with state L_e. Similarly, h_{JB} is the matrix element which describes how the vibration Q can mix the states $|J_e >$ and $|B_e >$ respectively and so are the other elements.

Now, after ball milling for several hours there are generation of vacancy induced defect states in the forbidden energy gap which is also to be incorporated in the vibronic functions. These defect levels may act as an electron sink, with a dual ability to trap and eject excitons to the matched levels. Here the defect states are denoted by $|V_e >$ in a similar fashion and h_{LV} and h_{JV} are similarly the matrix elements representing the degree of mixing between the vibronic states $|J_e >$, $|L_e >$ of the molecule to the defect energy states $|V_e >$ of the semiconductor.

For the purely electronic transition moment between states, we write:

$$M_{JL} =< J_e|\mu|L_e >, \quad M_{BL} =< B_e|\mu|L_e >, \quad M_{JC} =< J_e|\mu|C_e >,$$

$$M_{JV} =< J_e|\mu|V_e >, \quad M_{VL} =< V_e|\mu|L_e >. \qquad (16)$$

So, by substituting all these, the expression for the polarizability tensor $\alpha_{\sigma\rho}$ is derived as follows:

$$\alpha_{\sigma\rho} = A + B + C \qquad (17)$$

$$A = \sum_{L_e \neq J_e} \sum_k \left[\frac{M_{JL}^{\sigma} M_{LJ}^{\rho}}{\hbar(\omega_{LJ} - \omega_0)} + \frac{M_{JL}^{\rho} M_{LJ}^{\sigma}}{\hbar(\omega_{JL} + \omega_0)} \right] < j|l >< l|j > \quad (18)$$

$$B = \sum_{L_e \neq J_e} \sum_l \sum_{C_e \neq L_e} \left\{ \left[\frac{h_{LC} M_{JL}^{\sigma} M_{LJ}^{\rho}}{\hbar(\omega_{LJ} - \omega_0)} + \frac{h_{LC} M_{JL}^{\rho} M_{LJ}^{\sigma}}{\hbar(\omega_{LJ} + \omega_0)} \right] \frac{<j|l><l|Q|g>}{\hbar\omega_{LC}} + \right.$$

$$\left. \left[\frac{h_{LC} M_{JC}^{\sigma} M_{LJ}^{\rho}}{\hbar(\omega_{LJ} - \omega_0)} + \frac{h_{LC} M_{JC}^{\rho} M_{LJ}^{\sigma}}{\hbar(\omega_{LJ} + \omega_0)} \right] \frac{<j|Q|l><l|g>}{\hbar\omega_{LC}} \right\} + \sum_{L_e \neq J_e} \sum_l \sum_{V_e \neq L_e} \left\{ \left[\frac{h_{LV} M_{JL}^{\sigma} M_{VJ}^{\rho}}{\hbar(\omega_{LJ} - \omega_0)} + \right. \right.$$

$$\left. \left. \frac{h_{LV} M_{JL}^{\rho} M_{VJ}^{\sigma}}{\hbar(\omega_{LJ} + \omega_0)} \right] \frac{<j|l><l|Q|g>}{\hbar\omega_{LV}} + \left[\frac{h_{LV} M_{JV}^{\sigma} M_{LJ}^{\rho}}{\hbar(\omega_{LJ} - \omega_0)} + \frac{h_{LV} M_{JV}^{\rho} M_{LJ}^{\sigma}}{\hbar(\omega_{LJ} + \omega_0)} \right] \frac{<j|Q|l><l|g>}{\hbar\omega_{LV}} \right\} \quad (19)$$

$$C = \sum_{L_e \neq J_e} \sum_l \sum_{B_e \neq J_e} \left\{ \left[\frac{h_{JB} M_{JL}^{\sigma} M_{LB}^{\rho}}{\hbar(\omega_{LJ} - \omega_0)} + \frac{h_{JB} M_{JL}^{\rho} M_{LB}^{\sigma}}{\hbar(\omega_{LJ} + \omega_0)} \right] \frac{<j|l><l|Q|g>}{\hbar\omega_{JB}} + \right.$$

$$\left. \left[\frac{h_{JB} M_{BL}^{\sigma} M_{LJ}^{\rho}}{\hbar(\omega_{LJ} - \omega_0)} + \frac{h_{JB} M_{BL}^{\rho} M_{LJ}^{\sigma}}{\hbar(\omega_{LJ} + \omega_0)} \right] \frac{<j|Q|l><l|g>}{\hbar\omega_{JB}} \right\} + \sum_{L_e \neq J_e} \sum_l \sum_{V_e \neq J_e} \left\{ \left[\frac{h_{JV} M_{JL}^{\sigma} M_{LV}^{\rho}}{\hbar(\omega_{LJ} - \omega_0)} + \right. \right.$$

$$\left. \left. \frac{h_{JV} M_{JL}^{\rho} M_{LV}^{\sigma}}{\hbar(\omega_{LJ} + \omega_0)} \right] \frac{<j|l><l|Q|g>}{\hbar\omega_{JV}} + \left[\frac{h_{JV} M_{VL}^{\sigma} M_{LJ}^{\rho}}{\hbar(\omega_{LJ} - \omega_0)} + \frac{h_{JV} M_{VL}^{\rho} M_{LJ}^{\sigma}}{\hbar(\omega_{LJ} + \omega_0)} \right] \frac{<j|Q|l><l|g>}{\hbar\omega_{JV}} \right\} \quad (20)$$

The term A here represents the sole contribution of the molecular resonance to the polarizability tensor via M_{JL} and is not affected by the defect states in the semiconductor. Whereas, B represents the contribution of PICT from molecule to semiconductor to the polarizability tensor via M_{JC} and M_{JV}. The transition borrow intensity from the allowed transition M_{JL} by means of vibronic coupling between excited molecular state L and semiconductor band state C through the matrix element h_{LC}, similarly, the transition borrow intensity from the allowed transition M_{JL} by means of vibronic coupling between the excited molecular state L and the semiconductor defect state V through the matrix element h_{LV}.

Similarly, C represents the contribution of PICT from semiconductor to molecule to the polarizability tensor via M_{BL} and M_{VL}. The transition borrow intensity from the allowed transition M_{JK} by means of vibronic coupling between the molecular ground state J and the

semiconductor valence band state B through the matrix element h_{JB}, similarly, the transition borrow intensity from the allowed transition M_{JL} by means of vibronic coupling between the molecular ground state J and semiconductor defect state V through the matrix element h_{JV}. These calculations including the vacancy related trap states were followed from the work of Cong et al. following the SERS enhancement of defective WO_3.[24]

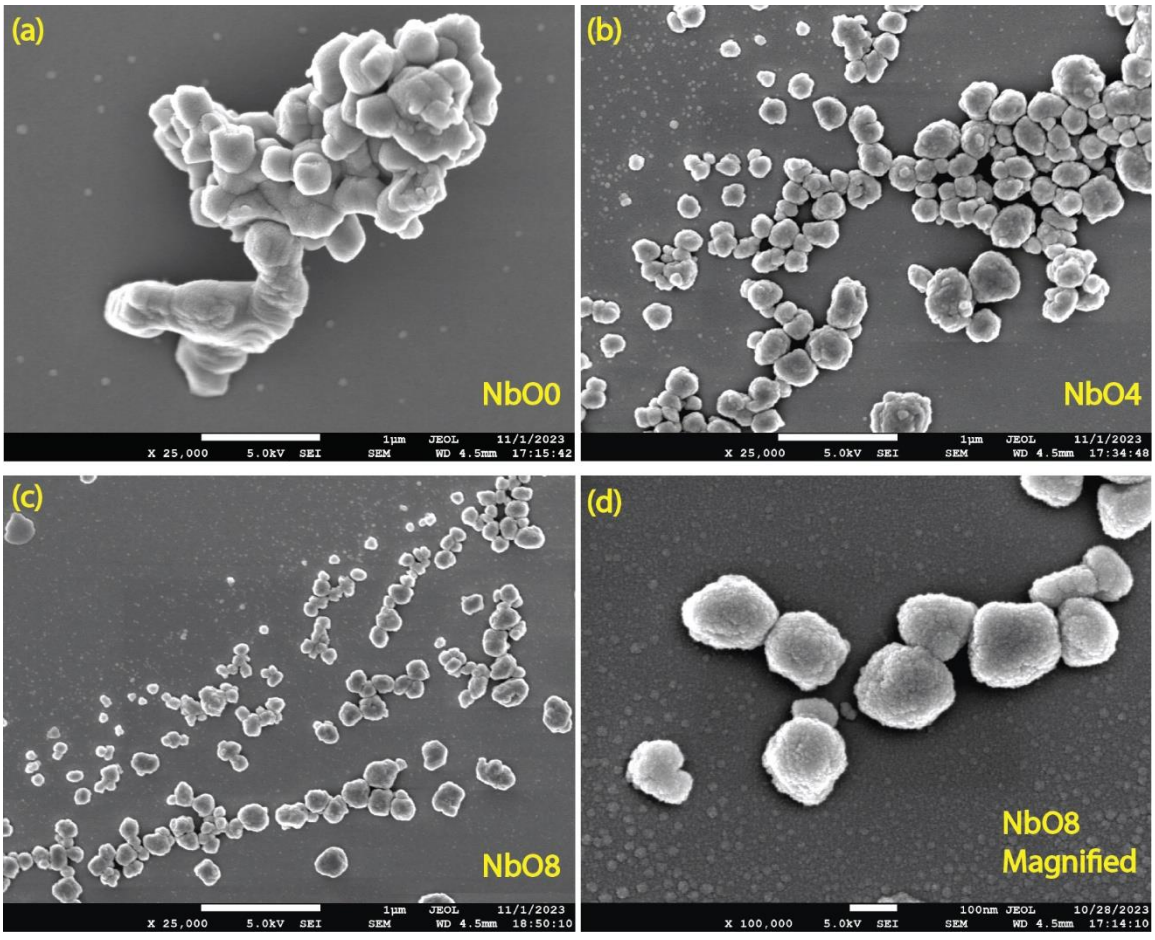

Fig. S8: Large area FESEM images of the Nb_2O_5 nanoparticles dispersed on the substrate after (a) 0 h, (b) 4 h, and (c) 8 h of milling. Scale bar in 1 μm in each case. (d) Magnified image (scale bar is 100 nm) of aggregated Nb_2O_5 nanoparticles after 8 h of milling, which is taken into account for the FEM simulation.

References:

(1) Bhakat, A.; Paul, S.; Chattopadhyay, A. Molecular Specificity in the Intense Surface-Enhanced Raman Scattering on Copper(II) 8-Hydroxyquinoline Microcrystals. *J. Phys. Chem. C* **2023**, *127* (10), 5169–5177.

(2) Cong, S.; Yuan, Y.; Chen, Z.; Hou, J.; Yang, M.; Su, Y.; Zhang, Y.; Li, L.; Li, Q.; Geng, F.; Zhao, Z. Noble Metal-Comparable SERS Enhancement from Semiconducting Metal Oxides by Making Oxygen Vacancies. *Nat. Commun.* **2015**, *6*, 1–7.

(3) Lombardi, J. R.; Birke, R. L. A Unified View of Surface-Enhanced Raman Scattering. *Acc. Chem. Res.* **2009**, *42* (6), 734–742.

(4) Shan, Y.; Zheng, Z.; Liu, J.; Yang, Y.; Li, Z.; Huang, Z.; Jiang, D. Niobium Pentoxide : A Promising Surface-Enhanced Raman Scattering Active Semiconductor Substrate. *npj Comput. Mater.* **2017**, No. March, 1–6.